INTERNATIONAL JOURNAL FOR NUMERICAL AND ANALYTICAL METHODS IN GEOMECHANICS
*Int. J. Numer. Anal. Meth. Geomech.*, **23**, 531–547 (1999)

# DEM SIMULATION OF GRANULAR MEDIA—STRUCTURE INTERFACE: EFFECTS OF SURFACE ROUGHNESS AND PARTICLE SHAPE

RICHARD P. JENSEN[1,*,†], PETER J. BOSSCHER[2,‡], MICHAEL E. PLESHA[3,§] AND TUNCER B. EDIL[2,¶]

[1]*Geological Engineering Program, University of Wisconsin-Madison, Madison, WI 53706, U.S.A.*
[2]*Department of Civil & Environmental Engineering and Geological Engineering Program, University of Wisconsin-Madison, Madison, WI 53706, U.S.A.*
[3]*Department of Engineering Physics and Geological Engineering Program, University of Wisconsin-Madison, Madison, WI 53706, U.S.A.*

## SUMMARY

An enhanced discrete element method for the numerical modelling of particulate media is presented. This method models a particle of general shape by combining several smaller particles of simpler shape, such as a circle, into clusters that act as a single larger particle. The clusters more accurately model the geometry-dependent behaviour of the particles, such as particle interlock and resistance to rolling. The method is implemented within the framework of an existing DEM program without the introduction of new contact or force algorithms. An extensive set of numerical 'experiments' is performed which demonstrate the method's effectiveness. The granular media–structure interface shear test simulations are performed using both clustered and non-clustered particles. The results indicate that the clustered particles undergo less rolling and provide for increased shear resistance of the medium. Copyright © 1999 John Wiley & Sons, Ltd.

Key words: discrete element; interface; particle roughness; particle shape; cluster; shear strength

## 1. INTRODUCTION

Deformation of soil–structure systems usually involves the creation of an interfacial shear or slipzone that is very close to the structure. This interface is often only a few particle diameters wide and has large localized strains.[1] For particulate media such as sand, the influence of individual particle rotations, relative grain displacement, and grain crushing on interface behaviour such as shear resistance and dilatancy are poorly understood. Presently, the basis for most

*Correspondence to: Dr. Peter J. Bosscher, Rm. 2218 Engineering Hall, Department of Civil and Environmental Engineering, University of Wisconsin, 1415 Engineering Drive, Madison, WI 53706, USA
†Graduate Student
‡Associate Professor
§Professor
¶Professor

Contract grant sponsor: National Science Foundation; contract grant number: CMS-9302281
Contract grant sponsor: Air Force Office of Scientific research; contract grant number: MIRP-93-0031
Contract grant sponsor: AASERT; contract grant number: F49620-94-1-0325

CCC 0363–9061/99/060531–17$17.50

*Received 30 June 1997*
*Revised 24 April 1998*

analysis and design of systems involving structure–particulate media interfaces is rooted in empirical relationships. In this paper we describe some enhanced numerical methods for modelling particulate media, and conduct an extensive series of numerical 'experiments' to help elucidate important phenomena in soil–structure interface behaviour.

Soil is inherently discontinuous and can be effectively modelled by the Discrete Element Method (DEM). This method was originally developed by Cundall[2,3] for modelling two-dimensional joined rock masses by idealizing a rock mass to consist of plane polygon-shaped rigid particles that interact along deformable frictional boundaries. In two dimensions, each particle brings three degrees of freedom to the model. The method was subsequently enhanced by Cundall and Strack[4–6] for applications to soils by idealizing a soil mass to consist of an assemblage of circular shaped rigid disks for two-dimensional idealizations, or spheres for three-dimensional idealizations. The rigid disks or spheres are usually very large in number, and interact through deformable frictional contacts with neighbouring particles.

Such an approach opens up pathways to new knowledge of particulate media because it is possible to observe and quantify phenomena and minute detail on a microscopic level. In contrast, laboratory studies are useful for providing macroscopic information on real materials, but resists attempts to glean microstructural information because of the difficulty in viewing and/or measuring phenomena that are interior to the specimen.

While modelling particulate media with discs or spheres is computationally simple, it has been found that the particles tend to roll or rotate excessively.[7] In order to reduce particle rotations to more realistic levels, some researchers have employed the ad hoc, and perhaps ill-founded practice of artificially constraining the rotations of particles periodically throughout the course of a simulation.[8] Comparison of numerical simulations with typical response of laboratory specimens shows that DEM simulations using simple discs or spheres usually underestimates the shear resistance of the medium when the medium is subjected to uniform compressive loading.

Many individuals have enhanced DEM to include particles with more complex shapes that more closely replicate those in natural media. Walton[9] and Issa and Nelson[10] employed arbitrary polygon-shaped elements that are reminiscent of those used in fractured rock mechanics and established that such an approach yields better qualitative agreement with experiments. However, such an approach has some computational disadvantages (e.g. the contact detection scheme may be time-consuming because of the large number of surfaces that require monitoring). In fact, Ting *et al.*[11] report at least one order of magnitude increase in execution time for simulations using polygon-shape particles compared to circular, or disc-shaped particles. Additional disadvantages arise from treatment of the vertices that are present in polygon-shaped particles. Ambiguities occur in specifying whether a contact should be treated as edge–edge, edge–corner, or corner–corner, and switching from one contact type to another is difficult. There is also no unique outward normal direction at a vertex. Furthermore, extension from 2-D to 3-D is much more complex in comparison to extensions using simple particle shapes.[2,7] In order to address these problems, Ting *et al.*[12] developed elliptically shaped particles and established that such an idealization better replicates the resistance of particles to rotation that is observed in natural media. Also, an elliptical particle has a unique outward normal direction, and has a surface that is represented by a single function. Disadvantages with elliptical particles is that the contact detection algorithm, while substantially faster than that for polygon shaped particles, is still not as efficient as those for simple circular disks and spheres. Also, extensions that might allow for modelling of additional details of particle roughness are not clear.

 

In this paper, we develop an idea for modelling rough particles based on *clustering*. A cluster is an assemblage of particles having simple shape. While this idea is probably not new, in this paper we thoroughly explore its utility and usefulness in modelling natural particulate media, and attempt to glean important information on the micromechanical aspects of particulate media deformation. Work related to clustering has been done by Trent and Margolin,[13] wherein they bond particles together to model fracture in cemented granular solids. Also, rigid clusters have been used by Walton and Braun[14] and Qiu and Kruse[15] to model particle flow in rotating drums and in conveyor transfer chutes, respectively. In Section 2, we provide a brief overview of DEM modeling. In Section 3, we describe clustering in detail and in Section 4, a periodic boundary treatment is described. The numerical simulations are described in Section 5 and the results of these simulations are thoroughly discussed in Section 6.

## 2. DISCRETE ELEMENT MODELLING

We have conducted our DEM modelling using a highly modified version of the program TRUBAL.[5,6] In this implementation of DEM, particles are modelled as rigid circular discs in 2-D or rigid spheres in 3-D. As shown in Figure 1, each interparticle contact is modelled with a normal-direction spring and dashpot, and a spring–dashpot–slider assembly in the tangential direction. The non-linear force-displacement relations are shown in Figure 2 in which it is seen that the normal direction behaviour is linear-elastic with a no-tension limit, and the shear direction behaviour is linear-elastic with a Coulomb friction limit. In 2-D, each particle has three degrees of freedom, two translational and one rotational. For many problems, the rate of loading is sufficiently high that inertial forces are important. However, even for quasi-static loadings, such as those considered in this paper, inertial forces are included in the discretization so that explicit time integration can be used to find a sequence of equilibrium solutions. If inertial forces are omitted, which is certainly warranted for the slow loading rates considered in this work, an implicit solution scheme would need to be used. But, implicit methods are difficult to implement and achieve convergence for problems that are as strongly non-linear as those considered here.

The equations of motion are integrated in time using the explicit central difference method. This method is easy to implement for non-linear problems such as this and is fairly robust and shows good accuracy, but is only conditionally stable. With no damping, the linearized time step stability limit is $\Delta t < 2/\omega_{\max}$ where $\omega_{\max}$ is the instantaneous highest natural frequency of

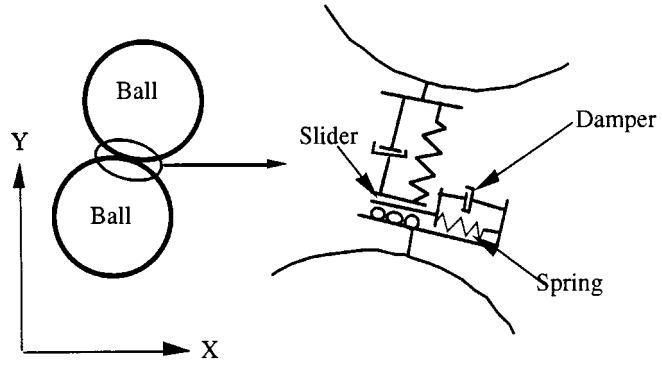


Figure 1. Particle contact model as idealized in DEM

 

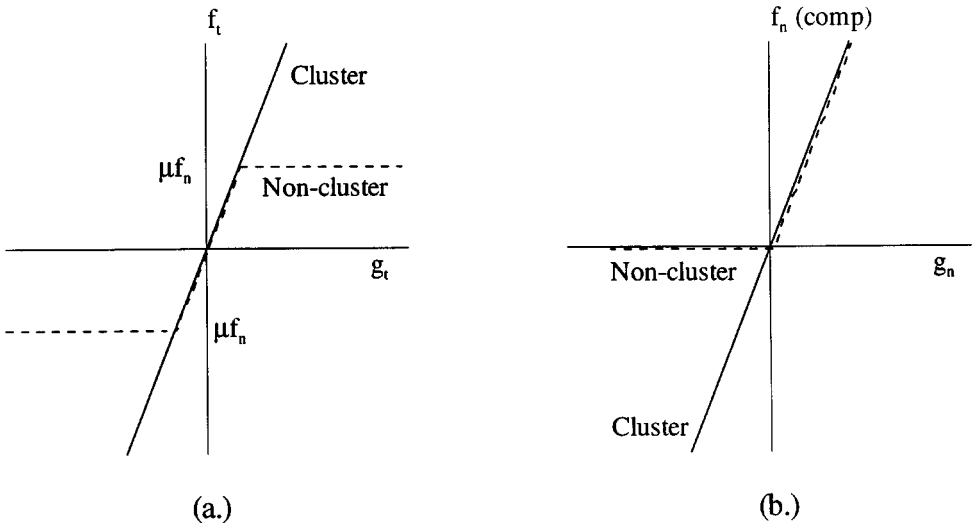


Figure 2. Interparticle load–displacement relationships. (a) The shear force load–displacement relationship. For the non-cluster particles, when the tangential forces reach $\mu f_n$ the particles slip perfectly plastically. No slip is allowed between the particles which make up the cluster. (b) The interparticle normal load–displacement relationship. No tension is allowed at contacts where non-clustered particles are involved

vibration for the system; see Cook *et al.*[16] In most implementations of explicit time integration, including TRUBAL, a global stiffness matrix is not formed and hence, computation or estimation of $\omega_{\max}$ is not possible. Furthermore, bounding of $\omega_{\max}$ using a Fried inequality is also not possible; see Reference 17. Thus, an ad hoc scheme for time step selection is used in TRUBAL wherein $\Delta t = \alpha\sqrt{m_{\min}/k_{\max}}$ in which $k_{\max}$ is the largest interparticle spring stiffness, $m_{\min}$ is the mass of the smallest particle, and $\alpha$ is user-selected parameter. Computational experience suggests that taking $\alpha$ to be of the order 0·1 is typically satisfactory to provide a stable computation. However, stability is not guaranteed by this criterion for all problems and it is quite possible to have a momentary instability that is subsequently arrested. Since no additional measures of solution stability, such as an energy balance, are implemented, users should be cautious of solution quality.

## 3. CLUSTERS

To model rough particles more naturally and effectively, we have developed the concept of a *cluster*. As shown in Figure 3(a), naturally occurring particles are rarely circular and a disc or sphere does not closely model reality. Figure 3(b) shows a circular particle superimposed on a natural particle. As a discrete model, the circle also does not capture the effects of the particle shape or the surface asperities of the particle. As previously discussed, modelling of natural particles using circular particles results in excessive particle roll and in inaccurate moment computation due to applied normal forces.[12]

By combining a number of simple circular-shape particles in a semi-rigid configuration, a better model of a natural particle is constructed. As seen in Figure 3(c), a number of particles

 

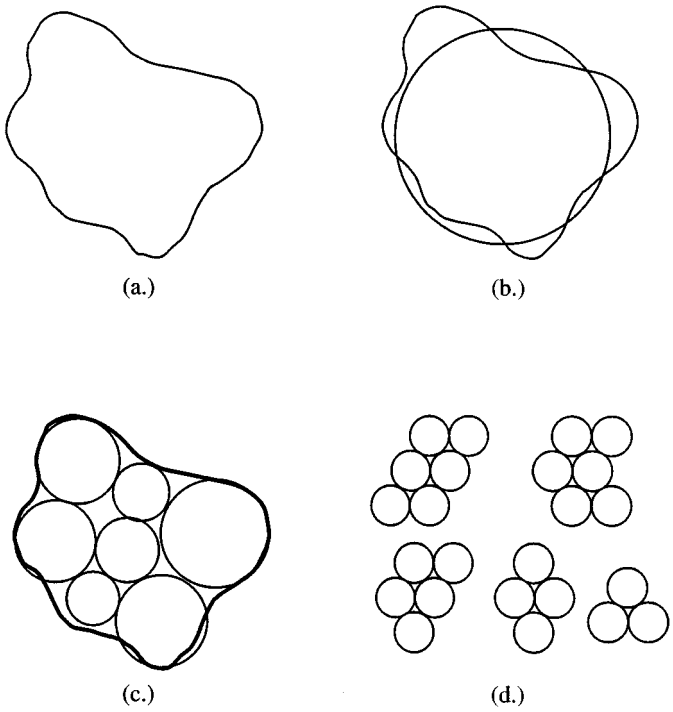


Figure 3. (a) Outline of sand particle. (b) DEM disc element superimposed over sand particle. As can be seen in this figure, the disc element does not model the geometry of an actual particle very closely. As a result, using discs results in excessive roll and inaccurate moment computations. (c) Any number of DEM particles are joined together in a rigid configuration, called a 'cluster,' which closely resembles the actual particle. The particles forming the 'cluster' rotate and translate as a rigid body. (d) 'Clusters' can be formed in any arbitrary combination and with any number of DEM particles. This figure shows several possible combinations. As a first step, the work done to this point uses 'clusters' composed of three DEM particles

can be joined together in a configuration that closely resembles an actual particle. Any number of particles may be linked together to form a 'cluster.' The only requirement is that the particles forming the 'cluster' rotate and translate essentially as a rigid body. Figure 3(d) shows examples ranging from three particles 'clusters' to different configurations of six particle 'clusters'.

To force the individual particles of a cluster to behave as a rigid body, the interparticle contacts within the cluster are constrained to be linear-elastic as shown in Figure 2. Hence, interparticle contacts within a cluster are allowed to support unlimited tension and shear force. One of the advantages to clustering is that the internal workings of TRUBAL remain unchanged in regard to contact detection (which is very efficient for circular-shape particles), time integration, and internal force computations (excepting very minor modifications to render cluster interparticle contacts to remain linear elastic). The program recognizes all of the particles that make up a cluster as a separate entity.

Clustering offers many features. One of them is to handle particles of potentially very complex shape, though in this paper we restrict our attention only to three-particle clusters as shown in Figure 4. Phenomena such as damage and grain crushing, which could not be explored by prior DEM approaches, can be easily investigated. In a subsequent paper, we investigate some

 

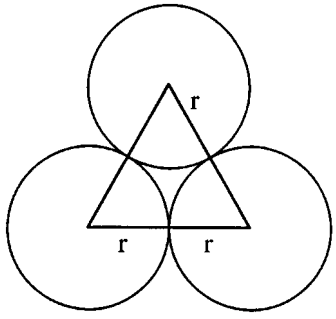


Figure 4. A simple three-particle 'Cluster'

objective criteria for grain crushing and the implications of this on shear zone formation and behaviour. Also, the simplicity and speed of the contact detection algorithms for simple-shape particles are retained. Extension to 3-D is very straightforward. The major disadvantage to clustering is a substantial increase in the number of degrees of freedom for a discretization. The circular or elliptical particles in DEM has three degrees of freedom (DOF). With clustering, each cluster has a total number of DOF equal to $3n_c$ where $n_c$ is the number of particles within a cluster. Thus, an equivalent cluster model for a medium would have about $n_c$ times the number of DOF as a model that uses just circular or elliptical particles. Considering that explicit time integration is used, this implies a roughly proportional increase in simulation time of about a factor of $n_c$ using serial computing. However, in the case of circular particles, the results of a cluster simulation should be substantially more accurate, while in the case of elliptical particles, it is expected that the simulation time would be partially compensated by the more efficient contact detection algorithm used by clustering. Also, there would perhaps be an improvement in accuracy since it is possible to more accurately model the shape and roughness present in natural particles.

## 4. PERIODIC BOUNDARIES

Because of limited computing capacity, the total number of particles that can be realistically used in a DEM simulation is small in comparison to the actual number of particles existing in any laboratory sample or actual engineering situation. In order to increase computing efficiency as well as remove any deleterious boundary effects, *periodic boundaries* are used. Campbell and Brennen[18] developed periodic boundaries for use in numerical simulation of granular shear flows. The periodic boundaries allow a particle to pass out of one side of the problem domain and automatically reappear on the opposite boundary such that truly periodic conditions are enforced. When the particle reappears at the opposite boundary, it has the same $y$-coordinate (see Figure 5) and velocity with which it left. Therefore, the control volume is infinitely replicated on both sides. This allows the side boundary condition to be infinite and thereby removes the unwanted influence of a nearby wall. In the DEM simulations where the number of particles is restricted due to computing capacity, removal of boundary effects of a wall greatly increases the accuracy of the solution.

For example in Figure 5(a) as particle $i$ passes out the right-hand side boundary, another particle with exactly the same motion is introduced at the left boundary. That is, when particle

 

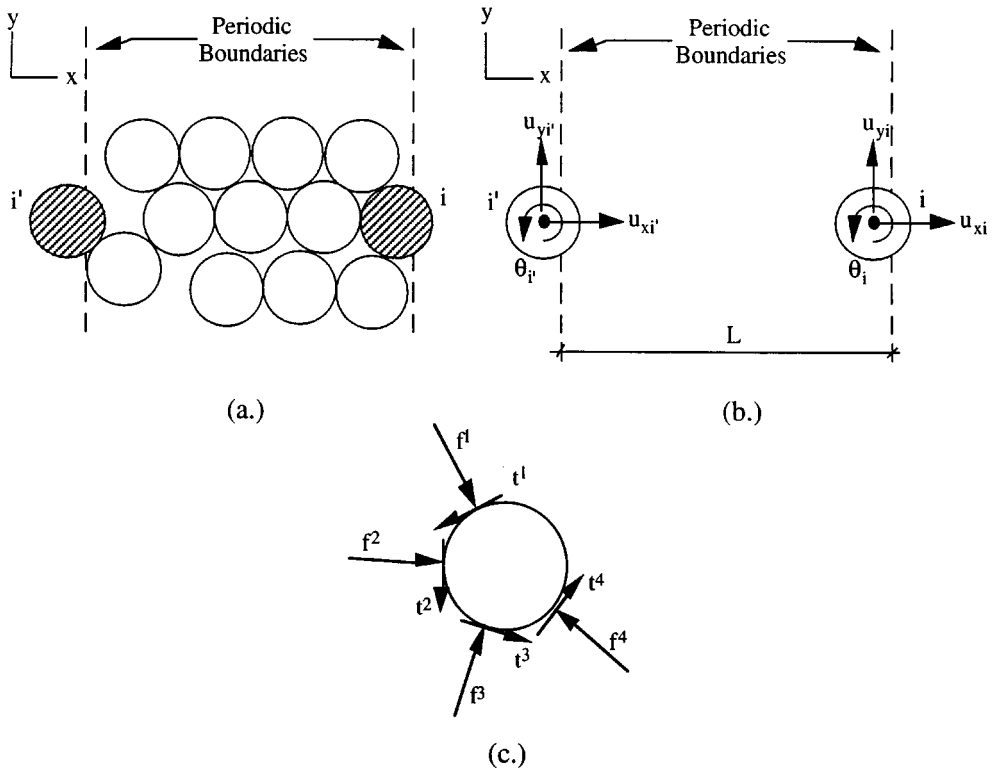


Figure 5. (a) Assemblage of circular particles with vertical periodic boundaries, (b) introduction of particle $i'$ at left-hand periodic boundary as particle $i$ leaves right-hand periodic boundary, (c) contact forces on particle $i$ which straddles a periodic boundary

$i$ first touches the right boundary (or left), a new particle is introduced at the left boundary (or right) with the same horizontal position, $y_1$, and with vertical position decremented by the period $L$. As particle $i$ straddles the right-hand boundary, its position is $x_1$, $y_1$ with total rotation $\theta_1$. The new particle $i'$ that was introduced at the left boundary has position $x_1 - L$, $y_1$ and rotation $\theta_1$. During this period of time, the particles have exactly the same kinematics ($u_{xi'} = u_{xi}$, $u_{yi'} = u_{yi}$, and $\theta_{i'} = \theta_i$). Also during this period particle $i$ and $i'$ are scanned for new contacts that might develop. Figure 5(b) shows the free body diagram for particle $i$ in which contact forces $f^1$, $t^1$ through $f^3$, $t^3$ are produced from contacts of particle $i$ with other particles near the right-hand boundary while contact forces $f^4$, $t^4$ are produced from contact with a neighbouring particle near the left-hand boundary.

## 5. NUMERICAL SIMULATION

Simulations (i.e. numerical experiments) were performed to demonstrate the effectiveness of clustered particles compared to simple circular particles and to investigate microstructural interface phenomena. The parameters that are varied in these simulations are the use of clustered particles versus non-clustered particles, the roughness of the shearing structure surface, and the

 

magnitude of the applied normal force. The simulations model a two-dimensional shear test where particles are first compacted into a domain, a constant normal stress is then applied to the mass of particles, and finally the bottom surface of the domain, which represents the rough surface of a structure, is displaced at a constant shear strain.

The non-clustered discretizations consists of 1000 simple circular particles and the clustered discretizations consist of 1000 three-particle clusters (Figure 4). The particles in the non-clustered sets are discs with a radius of $D = 4{\cdot}31$ length units. The clusters are comprised of three discs with the centre of each disc at the vertex of an equilateral triangle having sides of two times the radius of the discs. The discs in each cluster have a radius of 2·0 length units. This results in the radius of the circle circumscribing a cluster to be $D = 4{\cdot}31$ length units, i.e. equal to the radius of a non-clustered particle. In all cases, the particles in the non-clustered sets have the same material properties as the particles in the clustered sets. The mass density of each particle is 1·0 mass units per length unit cubed. The coefficient of friction at the contact between two particles or a particle and a surface is 0·4, similar to quartz particle–quartz particle surface friction.[19] The normal and shear stiffnesses at the contact between two particles, or a particle and a structure surface are $7{\cdot}5 \times (10)^8$ force units per length unit. These stiffnesses can be viewed as penalty numbers that enforce contact surface constraints consisting of impenetrability and presliding stick. In the limit in which these stiffnesses become infinite, the constraints are exactly enforced. For finite, but large stiffness values, the constraints are approximated and do have a small effect on the size of elastic deformations. However, for particulate media problems, the elastic deformations are almost always insignificant compared to sliding deformations and deformations arising from contact separation. The effects of contact stiffnesses on response of media with polygon-shaped particles has been thoroughly studied in Belytschko *et al.*[20]

The numbers for stiffness and mass are arbitrarily picked, but it is not expected that they change the dynamic characteristics of the problem for the following reason. The characteristic time scale for the medium is related to $\sqrt{(m/k)}$ where $m$ and $k$ are the mass and stiffness, respectively. Since we are integrating the equations of motion at very close to the stability limit for explicit time integration, and are shearing the surface wall uniformly at a slow rate (relative to $\sqrt{(m/k)}$ over the entire duration of the simulation, the time scale for the loading relative to the time scale for structure response remains constant regardless of the particular values of $k$ and $m$. This conjecture is supported by numerical experiments.

The non-clustered and clustered data sets were both generated in a domain that is initially 450 length units wide by 400 units high. The domain has a structure surface, or wall, on the bottom of the domain, periodic boundaries on the two vertical sides of the domain, and a horizontal surface at the top of the domain. The particles were then compacted by applying a normal force to the top surface, which acts as a rigid surface to constrain the particles within the domain. The domain can be viewed as simulating a two-dimensional vertical section in a ring shear test as opposed to a direct shear or a simple shear test because there are no vertical side boundaries but periodic boundaries. This compaction procedure generated clustered sets with an aspect ratio (length : height) of about 4 : 1 and non-clustered sets with an aspect ratio of about 3 : 1. The corresponding two-dimensional porosities were on the average 17 and 16 per cent for the clustered and non-clustered sets, respectively. The porosity of the clustered sets is calculated with the intracluster void being counted as solid. Examples of non-clustered and clustered sets can be seen in Figures 6 and 7, respectively. Three different normal forces are considered: $5{\cdot}0 \times (10)^7$ force units, $10{\cdot}0 \times (10)^7$ force units, and $20{\cdot}0 \times (10)^7$ force units. Each data set was initially compacted under the lowest normal force, $5{\cdot}0 \times (10)^7$ force units. On this initial particle structure, or fabric,

 

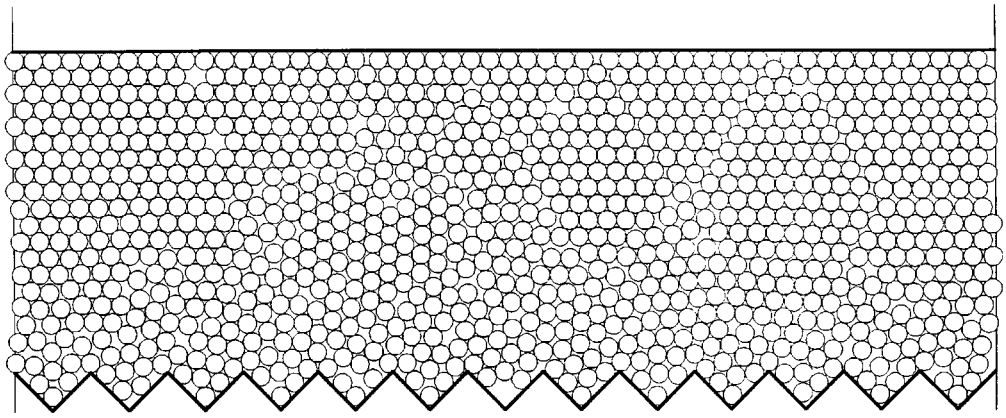

Figure 6. Compacted set of 1000 non-clustered particle. The sawtooth wall is the shearing surface. The sawtooth shown has a period of four times the diameter of the non-clustered particle, $\lambda = 4D$. Other simulation sets had shearing surfaces of $\lambda = 2D, 0{\cdot}5D$, and no sawteeth (but where the particles in contact with the shearing wall were fixed to the wall). The sets also had applied normal stresses, $\sigma_n = 5 \times (10)^7$, $10 \times (10)^7$, and $20 \times (10)^7$ units of stress. The side boundaries of all sets are periodic. Periodic boundaries allow particles that exit one side to reappear on the opposite side with the same position and velocity

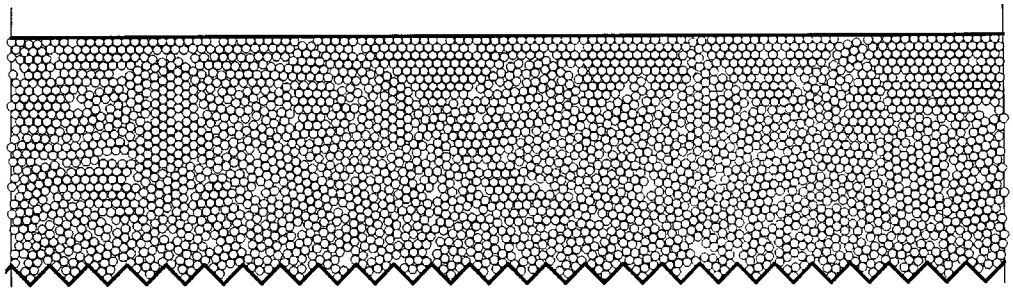

Figure 7. Compacted set of 1000 'clustered' particles (3000 DEM particles total). The shearing surface has a period of two times the 'cluster' diameter. The 'cluster' diameter is equal to the diameter of the non-clustered particles

the normal force was increased in a stepwise fashion, first to $10{\cdot}0 \times (10)^7$ force units, then to $20{\cdot}0 \times (10)^7$ force units. Applying the normal force increases in this fashion maintained the same basic particle assembly structure, thereby giving uniformity from simulation to simulation.

Several different cases were run for the clustered particles where all boundary conditions such as the geometry of the shearing surface and the applied normal stress were held constant while the packing arrangement of the particles was altered. The location of newly generated particles is based upon the random generation of locations within the specified domain. These locations are randomly generated from a program input seed value. By altering the seed, new configurations of particles were created. The results of these simulations showed that the general behaviour from run to run was the same in regard to shear stress and dilation as well as the average shear displacement and rotation of the particles. The shapes of the curves were all qualitatively similar with minor quantitative differences.

 

There are four different roughnesses of the shearing surfaces (i.e. structure surface) that are considered. These roughnesses are modelled using a sawtooth shape with different amplitude and period. The first of the four shearing surfaces is a straight wall with a coefficient of friction of 0·4 between the particles and the wall representing a 'smooth' surface. The remaining cases represent 'rough' surfaces and use a sawtooth surface with a slope of 45° with respect to the horizontal, and with periods (being defined as the distance from the top of one sawtooth to the top of the next sawtooth) of $\lambda = 4D$, $2D$, and $0{\cdot}5D$ where $D$ is as defined above. In the case of $\lambda = 4D$ (the roughest surface considered here), the period of sawtooth surface is four times the diameter of a cluster. The two finer surfaces have similar interpretations.

Once the sets have been compacted, the particles in contact with the top surface are glued to that surface. Hence, they have no rotation and no horizontal displacement, but do have the same vertical displacement as the top surface. This was done in order to ensure that the shear zone, if one forms, would be within the medium or near the shearing surface, rather than at this boundary. A total of 24 numerical simulations were performed from which comparisons and verifications of the procedure are taken. In addition, a numerical simulation was performed with a three-fold increase in the width of the domain and a subsequent increase in the total number of clustered particles. This additional run was performed to verify that the width of the domain was sufficiently large for accurate use of the periodic boundaries and that the results do not appreciably change with an increase in the domain size. This additional run also demonstrated that as the number of particles in contact with a rough structure surface increases, the smoothness of the shear stress versus shear displacement curves increases. A numerical simulation with a three-fold increase in the height of the domain was also performed. The results of this run showed no significant qualitative variation from the results of the standard domain. These additional runs verified that if the domain is of sufficient size, a varying aspect ratio should have little effect on the results of the numerical modeling.

## 6. DISCUSSION OF RESULTS

Four basic measurements have been extracted from the numerical simulations:

(1) the shear force required to displace the sawtooth shaped shearing surface,
(2) the dilation of the mass of particles which is measured by recording the normal displacement of the top wall,
(3) the particle displacements due to the displacement of the shearing force, and
(4) the rotation of the particles.

The particle displacement is measured as the change in the vertical and horizontal position of a particle with respect to its original position at the time when the shearing surface began displacing. The particle rotation is measured as the amount of rotation the particle undergoes from the time shearing surface displaces. The mass is divided into ten horizontal layers and the average displacement and rotation of the particles within each layer are computed. The applied force is proportional to an applied stress since the gross areas are the same in all simulations and will henceforth be referred to as a stress. Figure 8 is a montage of graphs showing the shear stress versus the tangential displacement of the shearing surface and the normal displacement of the top wall versus the tangential displacement of the shearing surface. Each graph in the montage contains three data sets that vary by the size of the applied normal stress. The three data sets use an applied normal stress of $5 \times (10)^7$ force units, $10 \times (10)^7$ force units, and $20 \times (10)^7$ force units,

 

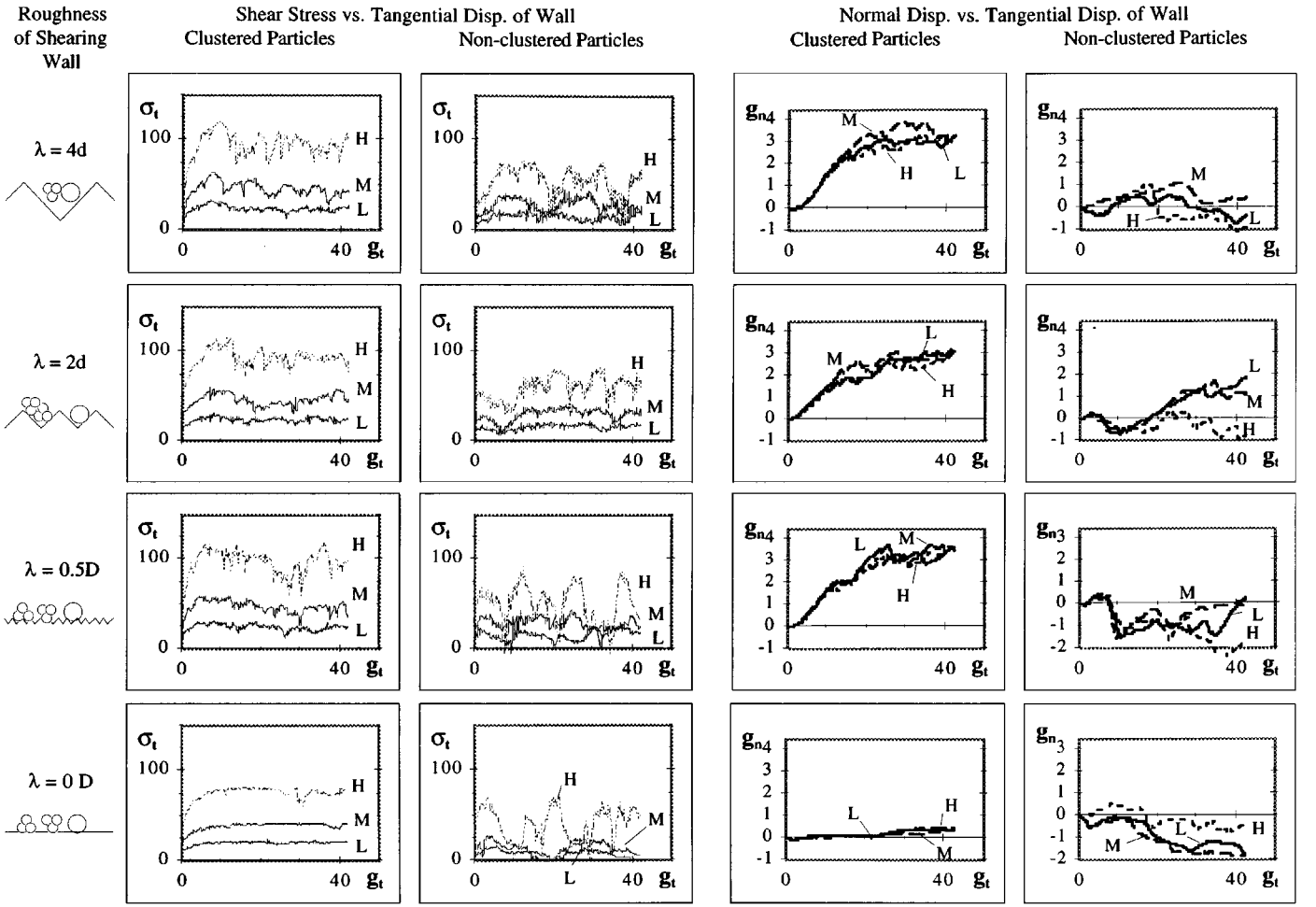


Figure 8. Graphs of Shear Stress at Shearing Wall versus Tangential Displacement of Shearing Wall and Dilation of Top Wall versus Tangential Displacement of Shearing Wall for all cases. Each graph shows the results of three different normal loadings. The cases are differentiated by **H**, **M**, and **L**. **H** represents the case with $\sigma_n = 20 \times (10^7)$, **M** is the case with $\sigma_n = 10 \times (10^7)$, and **L** is the case with $\sigma_n = 5 \times (10^7)$. In the Shear Stress versus Tangential Displacement graphs, the value of shear stress ($\sigma_t$) is in $10^5$ stress units. The values of shear displacement ($g_t$) and normal displacement ($g_n$) in all graphs are in length units

respectively. In each column of Figure 8, the graphs are grouped together as either clustered particles or non-clustered particles. The rows of the montage are grouped based upon the roughness of the shearing surface, with the top row having the greatest degree of roughness and the degree of roughness decreasing downward row by row. Figure 9 is a montage of the graphs showing the average displacement and average rotation in a layer versus the location of the layer. It is organized in the same manner as Figure 8 with the columns of graphs grouped according to whether the particles are clustered or not and the rows grouped according to the roughness of the shearing surface.

In all cases, the displacement that the shearing surface underwent was the same. The amount displaced was equal to about ten times the diameter of a clustered particle. The amount of shearing was decided based upon a reasonable number of time steps and achievement of steady-state stress–strain behaviour.

The shear stresses shown in the shear stress versus shear displacement plots of Figure 8 are compared by the summation of all horizontal force components that are in contact with the shearing surface. The relatively large fluctuations in the shear stresses seen as the shearing takes place could possibly be due to two related causes. The first is related to the number of particles used in the simulation. The contribution of each particle to the shear stress is summed for the total sawtooth surface. As particles make new contacts with the surface, and as particles lose contact with the surface, fluctuations in the stress are created. If too few particles are present, the contribution of each particle is a high percentage of the total, thus resulting in an abrupt fluctuation. A smoothing effect was seen in the trial run wherein the width of the domain and the number of particles were both increased by a factor of three. The second possibility is due to the stress networks in the medium building and collapsing as the surface shears. Walton[9] found fluctuations of $\pm 25\%$ for large particles, with the fluctuations being directly proportional to the size of the particle. The cluster particles seem to have a smaller fluctuation than the non-clustered particles, though not by a significant amount. This would conform to Walton's observation, since the mass and area of the individual particles in the clusters are smaller than those of the non-clustered particles.

Figure 8 shows that the shear stress versus horizontal displacement response of the cluster particle sets generated by displacing the sawtooth surface appear to have the same shape as would be expected for a medium packed sand of rounded sand grains (peak shear stress is the same or slightly higher than the steady-state (residual) shear stress.[21] The non-cluster sets have plots that are also similar in shape to the cluster sets but the shear stresses are somewhat lower than those of the cluster sets. The ratio of the maximum shear stress to normal stress can be viewed as the tangent of overall interface friction angle. The values obtained in the DEM analyses gave interface friction angles for the clustered sets comparable to those that would be expected between a well rounded, medium packed sand and a rough surface ($\sim 36^\circ$);[22] however, the values for the non-clustered sets were lower (see Figure 10). A problem associated with DEM models that use non-clustered discs to model particles is that the maximum shear stress to normal stress ratios of the modelled particle assembly is lower than what it should be, due to the excessive rotation of the particles.[12] The comparison of clustered and non-clustered sets herein support this explanation.

An important observation about the relation of shear stress to surface roughness can be seen from Figure 8. The peak shear stress of the 'rough' surfaces ($\lambda = 4D$, $\lambda = 2D$, and $\lambda = 0{\cdot}5D$), are essentially the same. Whereas, the peak shear stress of the 'smooth' surface ($\lambda = 0D$), is substantially less. If the roughness of the shearing surface is such that the particles can become engaged with the surface, the shear strength of the particle mass is determined by the particle-to-particle

 

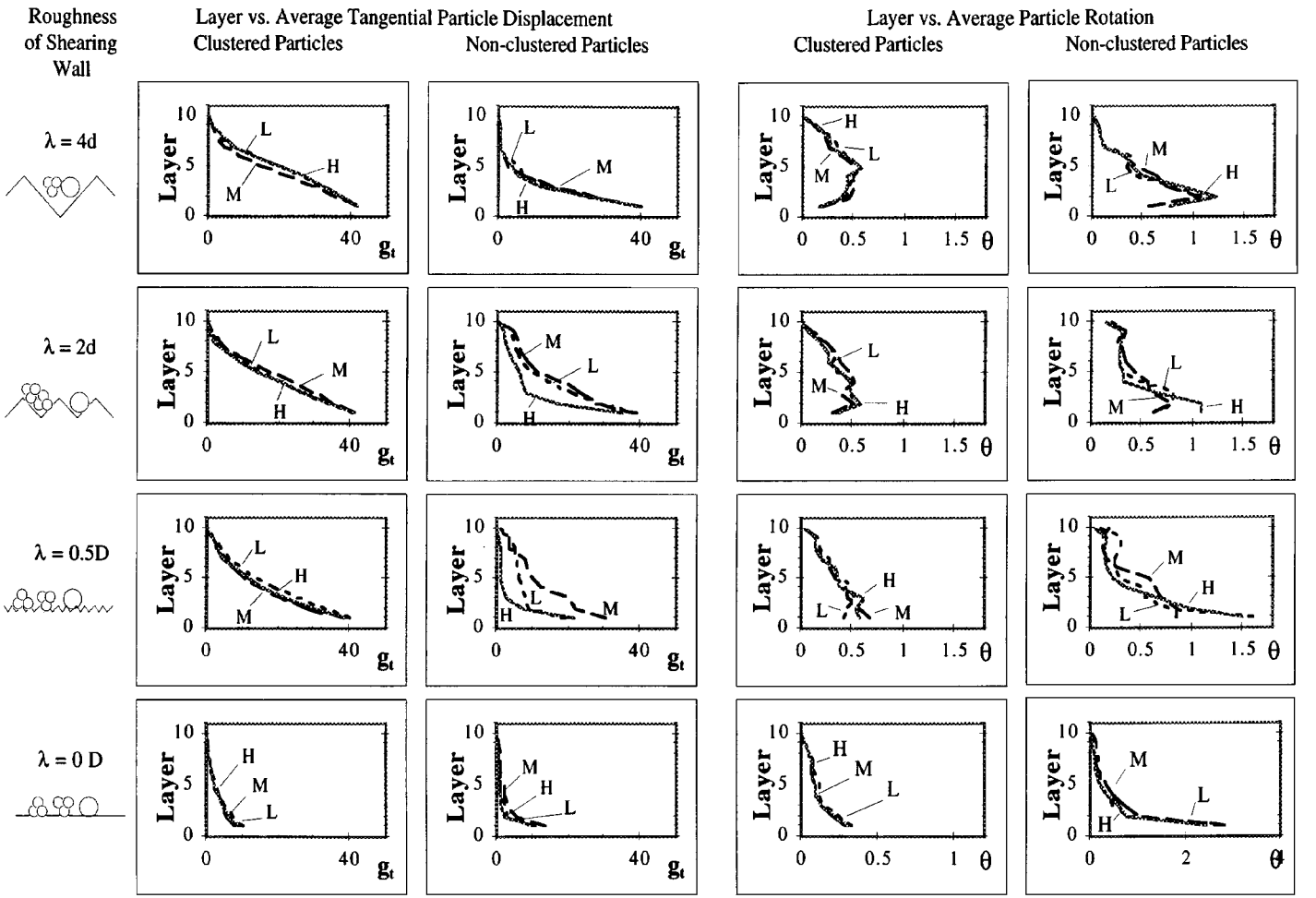


Figure 9. Graphs of Average Displacement by Layer versus Tangential Displacement of Shearing Wall and Average Rotation by Layer versus Tangential Displacement of Shearing Wall for all cases. Each data set is divided into 10 equal horizontal layers with layer number one adjacent to the shearing wall and layer number ten farthest from the shearing wall. The average displacement (or rotation) in a layer is the average displacement (or rotation) of all particles in that layer. The value of shear displacement ($g_t$) is in length units and the value of average rotation ($\theta$) is in radius

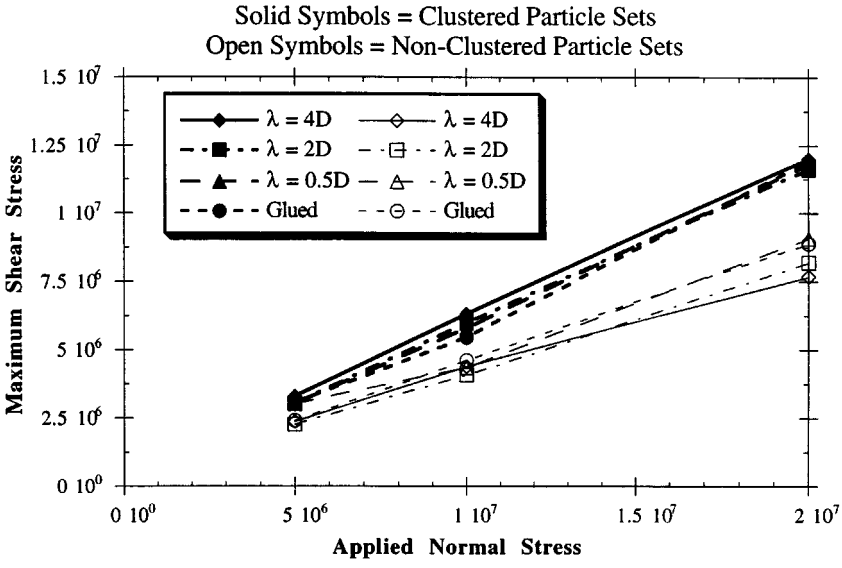


Figure 10. Graph of Maximum Shear Stress versus the Applied Normal Stress. For each data set, the maximum value of shear stress that was reached during shearing is plotted versus the applied normal stress

interaction in a zone adjacent to the shearing surface. If the shearing surface is sufficiently smooth such that the particles do not fully engage with the shearing surface, the shear strength is reduced to a simple frictional sliding problem between the particle mass and the smooth surface.

The dilation plots in Figure 8 indicate that the clustered particle sets have the same characteristics as a medium to densely packed sand. This is consistent with the corresponding shear stress plots. The dilation plots for the non-clustered particle sets are not as uniform or consistent. In all of the non-clustered particle sets, when the shearing begins, it acts as if it is a dense pack, initially compacting with subsequent dilation. Then, after a short period of dilation, it begins to compact again with varying amounts of compression and dilation. This effect could be caused by the high rotations present in the interface zone. Since the non-clustered sets have no interparticle locking, they will have a tendency to pack as densely as possible, with interparticle friction allowing for some dislocations. However, as the particles rotate, the rotations allow for the particles to overcome the interparticle friction and compact even more densely, after an initial period of dilation. As mentioned, dilation decreases after reaching a peak value in some of the non-cluster particle sets. Such a behaviour is not observed in the any of the clustered sets. For realistic DEM simulations of granular materials, this observation points out the importance of inclusion of interlocking features. Even though clusters are an improvement in realistic modelling of granular soils, improvements are needed relative to differentiating the effects of normal stress on dilation. The authors are endeavoring to resolve this by adding new features to the DEM code (e.g. grain crushing).

The depth versus average displacement plots in Figure 9 did not show a very definite interface zone for the clustered particle sets. While not linear, the curves indicate a fairly uniform change of displacement as the distance from the shearing surface increases. For the non-cluster particle sets, there was a very definite zone of localized displacement. The difference between the cluster and

 

the non-cluster cases may be due to the high rotations in the non-cluster medium. The formation of shear bands seems to relate closely to the particle freedom to rotate. The particles may be acting similar to roller bearings, allowing the larger mass of the specimen to displace much less than the shearing surface. It appears that the cluster particles are excessively interlocked such that minimal rotations occur. Thus, a well-defined shear band, as seen in the non-clustered particles, is not evident. To lend support to this explanation, a series of simulations were performed in which the rotations of non-clustered particles were severely restricted. A definite trend was observed that decreasing freedom to rotate causes more uniform distribution of displacements throughout the mass resulting in the lack of a distinct zone of relative displacement. The lack of a distinct zone of relative displacement in the cluster particle sets, may indicate that at the interface, the particle rotation is more important than the relative particle displacement.

The plots of the depth versus average particle rotation and the plots of depth versus average particle horizontal displacement seen in the montage of Figure 9 shows how the clustered particles reacted differently than the non-clustered particles. For all cases, a zone of higher particle rotation is evident. However, the average non-cluster particle rotation is nearly two times greater than the cluster rotation. This would seem to indicate that the clusters do in fact reduce the average particle rotation in DEM simulations. This is also confirmed by Figure 11, which shows the maximum average rotation plotted as a function of the applied normal stress. In all cases, the non-clustered particles had a higher average rotation than the clustered particles. Another item of note is that the rotations, in the simulations where the shearing surface is rough, $\lambda = 4D$ and $\lambda = 2D$, are smaller in the layer adjacent to the surface than in the layer second from the surface. This is in contrast to the simulations with the smoother shearing surfaces, $\lambda = 0{\cdot}5D$ and $\lambda = 0D$, in which the highest rotations in the layer are directly adjacent to the shearing surface. This can be explained by the particles in contact with the rougher surfaces being able to be fully engaged with the wall and thereby have their rotations subsequently reduced. In the case

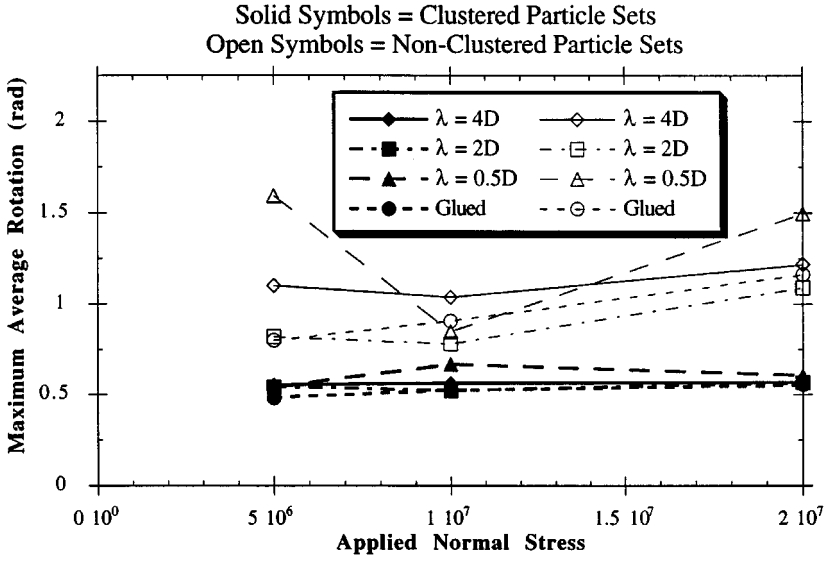


Figure 11. Graph of Maximum Average Rotation versus the Applied Normal Stress. For each data set, the maximum average particle rotation of any layer of the set is plotted versus the applied normal stress of the set

 

of the smoother shearing surface, the particles are larger than the sawtooth, therefore individual particles adjacent to the smooth surface are subject to less constraint than in the former case. This same phenomenon was seen by Tejchman and Wu[23] in the results of their finite element implementation of a Cosserat medium. They found that when they were modelling a sand-steel interface using Cosserat elements, the plots of the Cosserat rotation versus the height of the specimen for dense sand showed a very localized region of rotation. In addition, their two cases of the dense sand contacting (a) a very rough plate and (b) a moderately rough plate, were qualitatively identical to the plots of the non-clustered particles with a 'rough' and 'smooth' shearing surface.

A related observation from Figure 9 shows the influence that the degree of roughness of the shearing surface has on the location of the layer with the maximum average particle rotation. As the shearing surface becomes increasingly rougher, the layer of maximum average particle rotation moves farther from the shearing surface.

Figure 10 is a plot of the maximum shearing stress obtained during a shearing event versus the applied normal stress. This figure shows that the peak shear stress of the clustered particles is markedly higher than that of the non-clustered particles. A probable explanation for this is that due to the increased natural resistance to rolling of the clustered particles, as a result of their triangle profile, they are interlocking and forcing more particles to frictionally slide thereby increasing the resistance to shearing. This is supported by Figure 11, which is a graph of the maximum average particle rotation (as obtained from Figure 9) versus the applied normal force. This figure shows that the maximum average rotation in all of the non-clustered runs is markedly higher than that for the clustered runs. Therefore, it can be seen that an increase in shearing stress is accompanied by a decrease in the rotations of the particles.

## 7. CONCLUSIONS

An enhancement to the discrete element method for modelling particulate media has been presented. It has been shown that particles of general shape are effectively modelled by combining several smaller circular particles into a cluster that acts as a single larger particle. The creation of clusters can be done within the framework of existing DEM programs and without the need for new contact detection or force algorithms.

Numerical 'experiments' simulating ring shear tests were performed comparing the cluster particles to non-clustered particles. The 'experiments' were conducted with varying normal loads, roughness of the shearing surface, and particle types (clusters versus non-clustered). Periodic boundaries were used in order to increase the computing efficiency and to remove any deleterious boundary effects. The simulations clearly demonstrated that the particle rotations were significantly reduced when cluster particles were used as compared to the non-clustered particles. As a result, the shear strength of the cluster particle assembly is increased when compared to the non-clustered particle assembly.

Overall behaviour of the mass is qualitatively similar to those observed in experiments involving sands with round and angular particles. DEM revealed an intimate and detailed view of response at the particle level. In particular, the DEM simulations can be computer animated allowing enhanced visualization of all species of the particulate medium behaviour. A world-wide website (http:/bosscher.cee.wisc.edu), containing many of these animations is available.

Another feature of clustering is the opportunity to incorporate particle damage such as grain crushing, wear of roughness, etc. for more realistic simulation of particle medium. Research is currently in progress in this direction.

 

ACKNOWLEDGEMENTS

The contributions of Dr. Senro Kuraoka, Ms. Irina Dodoukh and Mr. Matthew A. Orzewalla are also gratefully acknowledged.

## REFERENCES

1. Z. Chen and H. L. Schreyer, 'Simulation of soil-concrete interface with nonlocal constitutive models', *J. Engng. Mech. Div*., ASCE **113,** 1665–1677 (1987).
2. P. A. Cundall, 'A computer model for simulation of progressive, large-scale movements in blocky rock systems', *Proc. Symp. Int. Soc. Rock Mech*., *Nancy*, II, Art. 8 (1971).
3. P. A. Cundall, 'A computer model for rock-mass behavior using interactive graphics for the input and output of geometric data', *Report AD/A-001.602* U.S. National Technical Information Service, 1974.
4. P. A. Cundall and O. D. L. Strack, 'The distinct element method as a tool for research in granular media, Part I', *NSF Report Grant ENG76-20711*, 1978.
5. P. A. Cundall and O. D. L. Strack, 'A discrete numerical model for granular assemblies', *Geotechnique*, **29,** 47–65 (1979).
6. P. A. Cundall and O. D. L. Strack, 'The distinct element method as a tool for research in granular media, Part II', *NSF Report Grant ENG76-20711*, 1979.
7. J. M. Ting, L. R. Meachum and J. D. Rowell, 'Effect of particle shape on the strength and deformation mechanisms of ellipse-shaped granular assemblages', *Engng. Comput*., **12,** 99–108 (1995).
8. R. Dobry and T. Ng, 'Discrete modelling of stress–strain behaviour of granular media at small and large strains', *Engng. Comput*. **9,** 129–143 (1992).
9. O. R. Walton, 'Particle-dynamics calculations of shear flow', in J.T. Jenkins and M. Satake (eds), *Mechanics of Granular Material: New Models and Constitutive Relations*, Elsevier, Amsterdam, 1982, pp. 327–338.
10. J. A. Issa and R. B. Nelson, 'Numerical analysis of micromechanical behaviour of granular materials', *Engng. Comput*., **9,** 211–223 (1992).
11. J. M. Ting, B. T. Corkum, C. R. Kauffman and C. Greco, 'Discrete numerical model for soil mechanics', *J. Geotech. Engng. Div*., ASCE, **115,** 379–398 (1989).
12. J. M. Ting, M. Khwaja, L. R. Meachum and J. D. Rowell, 'An ellipse-based discrete element model for granular materials', *Int. J. Numer. Anal. Meth. Geomech*., **17,** 603–623 (1993).
13. B. C. Trent and L. G. Margolin, 'A numerical laboratory for granular solids', *Engng. Comput*., **9,** 191–197 (1992).
14. O. R. Walton and R. L. Braun, 'Simulation of rotary-drum and repose tests for frictional spheres and rigid sphere clusters', *Joint DOE/NSF Workshop on Flow of Particulates and Fluids*, 20 Sept.–1 Oct 1993, Ithaca, NY.
15. X. Qiu and D. Kruse, 'Analysis of flow of ore materials in a conveyor transfer chute using discrete element method', *Joint ASME, ASCE, and SES Summer Meeting*, 29 June–1 Oct. 1997, Northwestern University, Chicago, IL.
16. R. D. Cook, D. S. Malkus and M. E. Plesha, *Concepts and Applications of Finite Element Analysis*, Wiley, New York, 1989.
17. M. E. Plesha, 'Eigenvalue estimation for dynamic contact problems', *J. Engng. Mech. Div*., ASCE, **113,** 457–462 (1987).
18. C. S. Campbell and C. E. Brennen, 'Computer simulation of granular shear flows', *J. Fluid. Mech*., **151,** 167–188 (1985).
19. P. W. Rowe, 'The stress-dilatancy relation for static equilibrium of an assembly of particles in contact', *Proc. Roy. Soc*., A **269,** 500–527 (1962).
20. T. Belytschko, M. E. Plesha and C. H. Dowding, 'A computer method for the stability analysis of caverns in joined rock', *Int. J. Numer. Anal. Meth. Geomech*., **8,** 473–492 (1984).
21. B. M. Das, *Advanced Soil Mechanics*, Hemisphere, New York, 1983.
22. Y. B. Acar, H. T. Durgunogly and M. T. Tumay, 'Interface properties of sand', *J. Geotech. Engng. Div*., ASCE, **108,** 378–398 (1982).
23. J. Tejchman and W. Wu, 'Experimental and numerical study of sand-steel interfaces', *Int. J. Numer. Anal. Meth. Geomech*., **19,** 513–536 (1995).

 